Submitted to TGARS

Experimental Verification of Ocean Bounced GPS Signals and Analysis of Their Application to Ionospheric Corrections for Satellite Altimetry

P. Axelrad[1], A. E. Cox, K. S. Crumpton
University of Colorado, Boulder

Abstract - An algorithm is presented which uses observations of Global Positioning System (GPS) signals reflected from the ocean surface and acquired by a GPS receiver onboard an altimetric satellite to compute the ionospheric delay present in the altimeter measurement. This eliminates the requirement for a dual frequency altimeter for many Earth observing missions. A ground-based experiment is described which confirms the presence of these ocean-bounced signals and demonstrates the potential for altimeter ionospheric correction at the centimeter level.

I. Introduction

In 1991, engineers at Dassault Electronique tested a GPS-based vehicle tracking system for range safety [1]. The system was installed on an Alfajet using a wrap-around antenna mounted in the nose of the aircraft. During a turn, the GPS receiver momentarily lost lock on one of the four satellites it was tracking. After re-acquisition, the GPS solution was in error by more than 100 meters. Post-processing of the GPS data revealed a discontinuity of approximately 1300 meters in the pseudorange measured from one particular satellite. Auber, et al. attributed this difference to the receiver locking on to a GPS signal reflected from the ocean instead of the direct signal from the satellite [1]. A similar phenomenon was noted by

[1] Corresponding Author - P. Axelrad, University of Colorado, CB 431, Engineering Center, ECNT 323, Boulder, CO 80309. Phone 303-492-6872, Fax 303-492-2825, E-mail Penina.Axelrad@Colorado.Edu

researchers from the Jet Propulsion Lab in tests conducted in Hawaii [2]. Based on these observations and their own theoretical development, Katzberg and Garrison [3] have suggested that a GPS antenna mounted on the nadir face of an altimetric satellite could be used to intentionally receive GPS signals reflecting from the ocean surface. They propose to use these signals to calculate and correct for the ionospheric delay of the altimeter measurements.

The use of altimetric satellites to measure topographic and geodetic features has grown in recent years with increasingly demanding accuracy requirements. Applications such as the study of oceanographic features require sea surface height measurement accuracy on the order of a few centimeters. Errors in orbit determination have now been significantly reduced leaving the delay due to the ionosphere as one of the largest error sources in a single frequency altimeter [4]. The magnitude of the ionospheric delay varies from about 0.2 cm to 20.0 cm for an altimeter operating at 13.6 GHz [4]. Current methods of correcting this error are either to use a dual frequency altimeter as on the TOPEX/POSEIDON satellite or to use values computed from ionospheric models. Dual frequency altimeters are considerably more expensive, consume more power, and are heavier as they are essentially two single frequency altimeters. Empirical models are plagued by their lack of coverage and the uncertainty in the ionosphere due to variations in solar activity, latitudinal dependencies, spatial variations, and other factors.

Signals from GPS satellites, at the L1 frequency of 1.575 GHz, are also delayed as they pass through the ionosphere and troposphere. In GPS applications, ionospheric corrections are computed based on dual frequency observations or a model, in much the same way as they are in altimetry measurements. In fact, GPS has been used to study both the ionosphere and the

troposphere by modeling these delays as a function of the atmosphere's structure. GPS-MET is a satellite experiment which measures additional tropospheric delays as the signal path from a GPS satellite to an observing, low-Earth-orbiting (LEO) satellite is occulted by the Earth's atmosphere [5]. If the positions of both the GPS satellite and the LEO satellite are known, the geometric path of the signal can be computed and any additional measured delays can be attributed to ionospheric and/or tropospheric delays.

Katzberg and Garrison [3] propose to use GPS signals reflected from the ocean surface arriving at an altimetric satellite for ionospheric calibration, as illustrated in Figure 1. This is accomplished by using a nadir-mounted GPS antenna to track reflected signals from GPS satellites which are within a few degrees of the altimetric spacecraft zenith. These signals travel through much the same ionosphere and troposphere below the altimetric satellite as the altimeter signals do. Since the position of the altimetric satellite is determined to high accuracy using measurements from a zenith mounted GPS antenna, and the GPS satellite positions are also determined to high accuracy, the geometric path of the bounced signal is very well known. The excess delay measured using the GPS C/A or P code can be attributed to ionospheric and tropospheric effects. Furthermore, the wet tropospheric delay in the bounced signal can be determined using the altimeter's radiometer [4]. The dry tropospheric delay may be reliably modeled. Thus, we find the potential to use bounced GPS measurements to identify the characteristics of the ionosphere in the region below the altimeter.

The purpose of this research is to confirm the reception of GPS signals reflected from the ocean; to quantify the accuracy of their measurement; and to extrapolate this information to an

expected accuracy for ionospheric calibration of an altimetric satellite. A ground-based experiment was conducted on an offshore platform to gather reflected and direct GPS signals for further analysis. The remainder of this paper is organized as follows: Section II describes the GPS observables and illustrates how combinations of these measurements may be used to calibrate the ionospheric delay in altimetry measurements. Section III describes the expected power levels and polarization of the reflected signals. Section IV describes the experiment conducted on an offshore platform and discusses the results obtained. The paper concludes with some comments on the implications of this experiment and plans for future experiments.

II. GPS Observables and Calibration of Ionospheric Delay

In general, the direct pseudorange (PR) observable from a GPS satellite to an observer is given by:

$$PR = \rho + b + SA + O + I + T + \varepsilon \tag{1}$$

where b refers to the receiver clock bias, SA refers to errors due to selective availability and GPS satellite clock error, O refers to range prediction errors produced by errors in the broadcast ephemeris, I is the ionospheric delay, T is the tropospheric delay, and ε refers to errors such as multipath and receiver noise [6]. The geometric range, ρ is computed based on the known position of the observer and the satellite position as determined from the broadcast or precise GPS ephemeris.

It is common in GPS to form a single difference between the pseudoranges to a satellite made by two different receivers. This cancels out errors due to SA and any ionospheric and tropospheric delays common to both. The single difference is given by:

$$\Delta PR = \Delta\rho + \Delta b + \Delta O + \Delta I + \Delta T + \Delta\varepsilon \qquad (2)$$

If both signal paths are approximately the same, the differential errors due to the orbit (ΔO), ionosphere (ΔI), and troposphere (ΔT) can be set to zero in Equation 2. If the same receiver or two synchronized receivers are used to make the two measurements, the differential clock bias (Δb) is zero.

For the receiver configuration onboard an altimetric satellite illustrated in Figure 1, the pseudorange measured by the zenith antenna corresponds to a direct range to the GPS satellite and the nadir antenna measurement would be a reflection. The geometric range, ρ of the reflected signal is computed by finding the distance between the GPS satellite and an image of the receiver located directly below the reflecting surface. Using synchronized receivers, the single difference observable between the antennas is given by:

$$\Delta PR = \Delta\rho + \Delta I + \Delta T + \Delta\varepsilon \qquad (3)$$

Solving Equation 3 for ΔI gives a measurement of the ionospheric delay below the altimetric satellite for the GPS frequency. Referring to this measured delay as ΔI_{GPS} to emphasize its dependence on the GPS frequency, it may be related to the ionospheric delay in the altimeter measurement I_{ALT}, as follows:

$$I_{ALT} = \frac{f_{GPS}^2}{f_{Alt}^2} \frac{\Delta I_{GPS}}{\gamma} \tag{4}$$

where f_{GPS} and f_{ALT} are the GPS and altimeter transmission frequencies, respectively, and γ is a geometrical scale factor. The simplest model for γ is $1/\sin\theta$, where θ is the GPS satellite elevation angle.

Thus, the accuracy with which the altimeter delay can be calculated is a function of the measurement and prediction accuracy of the GPS single difference. Using values from the TOPEX/POSEIDON altimetry satellite, an error of 2 m in the computation of ΔI_{GPS} produces an error of 2 cm in I_{ALT}.

An important goal of the ground experiment is to quantify the accuracy achievable for ranging with reflected GPS signals. In this case there were two independent receivers located approximately 40 m above the ocean surface. The single difference pseudorange for one GPS satellite is given by

$$\Delta PR = \Delta\rho + \Delta b + \Delta\varepsilon \tag{5}$$

where the differential errors due to orbit, ionosphere, and troposphere are all zero, but there is a remaining differential clock bias. This term is removed by double differencing the observations between two different GPS satellites:

$$\nabla\Delta PR = \nabla\Delta\rho + \nabla\Delta\varepsilon \tag{6}$$

Thus, using data from the ground experiment one can quantify the accuracy for ionospheric calibration, by analyzing the difference between $\nabla\Delta PR$ and $\nabla\Delta\rho$. The accuracy is limited by the knowledge of the geometrical path difference, $\nabla\Delta\rho$, which is based on the assumed antenna and GPS satellite positions, and $\nabla\Delta\varepsilon$ which includes multipath and receiver errors.

III. GPS Signal Strength and Antenna Design

Katzberg and Garrison [3] analyze the signal characteristics expected for GPS signals reflected from the ocean surface and received at some height above the ocean, including both power levels and polarity. GPS signals direct from the GPS satellites are right-hand circularly polarized (RCP) arriving at the Earth's surface with a nominal power level of -130 dBm. After correlation in a typical receiver this is seen as a carrier-to-noise power spectral density (C/N_0) in the range of 35-45 dB-Hz depending upon the receive antenna pattern and the receiver front end electronics. GPS signals reflected from the ocean surface will have varying polarization, predominantly left-

hand circularly polarized (LCP), and will lose phase coherence resulting in a high degree of variability in the received C/N_0. The overall power level should remain in the same range.

Figures 2 and 3 illustrate antenna gain patterns for a commercial RCP GPS antenna and a prototype LCP antenna constructed at the University of Colorado. The antenna gain patterns are shown for both RCP and LCP signals. Note that the commercial RCP antenna has some reception of LCP signals, although at a lower signal level and in a more random fashion. The same is true for the LCP antenna reception of RCP signals. This is critical information to identify the possibility of interference between the direct and reflected signals.

IV. Ground Experiment

The objectives of the ground experiment were to quantify the signal strength and measurement accuracy for GPS signals reflected off the ocean. We collected GPS carrier to noise ratios (C/N_0) and pseudorange measurements for as many satellites as possible using a variety of antenna configurations. A control receiver was set up to continuously monitor the direct GPS signals. Broadcast GPS orbits were used to compute the predicted geometric range double differences.

The experiment was conducted on March 26-27, 1996 on the Harvest oil platform, located off the California coast, near Point Conception. Platform Harvest was chosen for the following reasons -- 1) it is near sea water with a wide, unobstructed view of the ocean; 2) there is access to a test area 40 meters above sea level, which yields an observable path length difference between direct

and reflected signals; and 3) it has several GPS surveyed reference points. Figure 4 shows a sketch of the Harvest platform and identifies the data collection location.

The test equipment consisted of two 12-channel NovAtel 951R model GPS receivers [NOV], two computers for controlling the receivers and logging data, two standard RCP antennas (NovAtel Model 501), two LCP antennas, and a monopole antenna. Both of the receivers were configured to record raw satellite observations including pseudorange and C/N_0, without solving for position. One receiver and a zenith-pointed RCP antenna were established as a control to continuously record direct GPS signals. The second receiver, designated as the "test" was connected to one of the three remaining antennas, in various orientations, to track direct and reflected signals. All of the antennas have gain patterns which are preferential along the boresite direction; thus, the orientation of the test antenna was adjusted to attempt to track reflected signals. The antennas were mounted on a metal railing approximately one meter above the surface of the platform level. No antenna ground planes were used.

A total of eight separate experiments were conducted using this equipment in various configurations. No useful results were obtained with the monopole and one of the LCP antennas. The three remaining data sets, labeled A, B, and C were conducted using a prototype LCP antenna. The gain patterns for this antenna are shown in Figure 3 and details of the three data sets are given in Table 1. In the three data sets, a total of 16 satellites were tracked. The following sections discuss the experiments and several illustrative examples of the results.

Table 1: Harvest Data Set Summary

Data Set:	A	B	C
Date	27 Mar 96	27 Mar 96	27 Mar 96
Setup 1 Elevation: Azimuth	1554 PST (LCP) -45° 226°	1509 PST (LCP) +90°	0744 PST (LCP) -40° 226°
Setup 2 Elevation: Azimuth:		1515 (RCP) +90°	0800 (LCP) -60° 226°
Setup 3 Elevation: Azimuth:		1520 (LCP) -70° 226°	0815 (LCP) -30° 226°
Stop Time (PST)	1604	1530	0832

In Data Set A the LCP antenna was pointed at a constant angle of 45° below the horizon and an azimuth of 226°. At this time, Satellite Vehicle (SV) 39 was visible at an elevation of about 50° and an azimuth of 225°. SVs 34 and 35 were also visible as shown in Figure 5. The C/N_0 plots for all three satellites as seen by both the control and test antennas are shown in Figure 6. The measured and computed double differences between SV 39 and each of the other two are shown in Figure 7. The C/N_0 plots confirm that the SV 39 signal was a reflection because of the high signal level and the large amplitude oscillations relative to the control antenna signal. The C/N_0 for SVs 34 and 35 indicate that they are direct signals arriving at the test antenna. Figure 7 shows a disparity of 5 m between the measured and predicted double differences, out of a total double difference value of 50-65 m. This additional 5 m can be attributed to the interference of a direct signal into the backlobe of the antenna [7]. As shown previously in Figure 3, the RCP gain at 170° off boresite (at the back of the LCP antenna) is about -12 dB relative to the LCP gain on boresite.

In Data Set B the test receiver was switched between the RCP and LCP antennas in different orientations to demonstrate the acquisition and tracking of reflected signals. Three satellites, SVs 35, 39, and 24, were visible for this test as shown in Figure 5 with SV 39 at an elevation of 60° and an azimuth of 255° and SV 24 at an elevation of 55° and an azimuth of 175°. Data set B begins with the LCP test antenna pointed at zenith. Six minutes into the run, the test receiver was switched to a zenith pointing RCP antenna (minutes 6 to 11). Then after five minutes the test receiver was reconnected to the LCP antenna pointed down at an angle of 70° below the horizon. The poor reception of the direct signal by the LCP antenna can be seen in the C/N_0 plot of SVs 39 and 24 (Figure 8) during the interval of 0 to 5 minutes. During the second interval, the signal levels for both satellites go up by about 10 to 15 dB-Hz as soon as the RCP antenna is introduced. In the final phase of the data set (minutes 10 to 20) the C/N_0 values for the LCP antenna show high values with large fluctuations on the order of 10 to 15 dB-Hz, indicative of reflected signals. The direct signal from SV 35 was tracked throughout the test with much lower signal levels for the LCP antenna. Double differences for (SV 39 - SV 35) and (SV 24 - SV 35) are shown in Figure 9. The double difference values are near zero when two direct signals are tracked and approximately 60 m with one direct and one reflected signal. The disparity between the measured and computed double differences is approximately 5 m. Again, this can be attributed to the interference of a direct signal arriving at a backlobe of the antenna at about - 15 dB.

Table 2 summarizes the double difference results for all three of the key data sets. The maximum error between the measured and computed double difference is 8 meters and it appears as a slowly changing bias. This type of error could potentially be due to GPS orbital error, an

error in the assumed location of the antennas, or multipath interference. Because the antennas are only 2 meters apart, positioning errors cannot explain the up to 8 meter discrepancies. Furthermore, these errors would be consistent between the different data sets which we did not observe to be the case. We believe that the discrepancy is caused by direct signal interference on the reflected signal tracking.

Table 2. Summary of Double Difference Errors

Data Set	SV (Bounce)	SV (Direct)	Error (Measured - Computed) (meters)
A	39	35	4.4
A	39	34	4.7
B	39	35	5.3
B	39	37	5.4
B	24	35	4.4
C	13	18	6.0
C	14	18	7.3
C	14	28	7.7

In typical GPS applications, reflected signals, termed multipath, produce errors in the pseudorange observable by distorting the correlation function of the received signal. An expression given by Braasch [9] and shown in the Appendix (Equation A1), enables the computation of the tracking error as a function of the relative signal strength and delay. In this application, for the downward looking antenna, the reflection is the desired signal. The presence of the direct GPS signal produces an interference, the amplitude of which is determined by the gain pattern of the antenna. Looking at Data Set B, when the test antenna was pointed downward at 70° below the horizon, the direct GPS signal would hit the antenna at an angle of 145° relative to the boresite. This direct RCP signal acts like an interference at approximately -15 dB below

the desired signal (see Figure 3). According to equation A1, the maximum ranging error for this multipath interference, for a path length difference of 60 m, is 7 m. This is on the order of the disparity between the measured and computed double differences. Because of the requirement for double differencing we are actually combining four GPS signals, only one of which is a reflected signal. Each of the direct signals might also experience multipath interference due to GPS reflections from Platform Harvest or the ocean surface.

V. Conclusions

This paper presented an approach for using ocean reflected GPS signals to correct the ionosphere delay for altimetric satellites. An experiment at Harvest Platform verified the reception of these bounced signals and quantified the measurement accuracy in the range of 1-8 meters. An improved antenna design including a ground plane would reduce the possibility of signal interference which caused the largest of these errors. If ranging errors can be kept below 2 meters, the ionospheric calibration may be accomplished at the 2 cm level. Currently tests are being conducted at NASA Langley Research Center on a Boeing 737 [9]. Two receivers are being used connected to an RCP antenna on the top of the aircraft and an LCP antenna on the underside. Receiver modifications are also being studied to better track the reflected signals. The next step in evaluating this methodology is a spacecraft flight test.

References

1) J. Auber, A.Bibaut, J. Rigal, "Characterization of Multipath on Land and Sea at GPS Frequencies", ION GPS-94, Salt Lake City, Utah; pp. 1155-1171, September 20, 1994.

2) Sien-Chong Wu, T. Meehan, L. Young, "The Potential Use of GPS Signals as Ocean Altimetry Observables", ION GPS-97, Santa Monica, CA, January 14-16, 1997.

3) S. Katzberg, J. Garrison, "Utilizing GPS to Determine Ionosphere Delay over the Ocean", NASA TM 4750, December 1996.

4) U.S. World Ocean Circulation Experiment (WOCE) Technical Report Number 2, WOCE/NASA Altimeter Algorithm Workshop, Corvallis, Oregon, August 24, 1987.

5) K. Hardy, G. Hajj, E. Kursinski, "Accuracy's of Atmospheric Profiles Obtained from GPS Occultations", Proceedings of the ION GPS-93, Vol. II, Salt Lake City, Utah, pp. 1545-1556, September 22, 1993.

6) Parkinson, B.W., "GPS Error Analysis", Chapter 11, Parkinson, B.W., Spillker, J., Jr., Axelrad, P., and Enge, P. (eds.), *The Global Positioning System: Theory and Applications*, Volume I, AIAA, Washington, D.C., 1996, pp. 469-483.

7) Braasch, M.S., "Multipath Effects", Chapter 14, Parkinson, B.W., Spillker, J., Jr., Axelrad, P., and Enge, P. (eds.), *The Global Positioning System: Theory and Applications*, Volume I, AIAA, Washington, D.C., 1996, pp. 547-568.

8) W. Lippincott, T. Milligan, D. Igli, "A Method For Calculating Multipath Environment and Impact on GPS Receiver Solution Accuracy", Proceedings of the ION-96 National Technical Meeting.

9) J. Garrison, S. Katzberg, "Detection of Ocean Reflected GPS Signals: Theory and Experiment", submitted to IEEE SouthEastCon, 12 April 1997.

Appendix A

This experiment involved looking at the direct signal as the interfering multipath signal. This interference will result in a pseudorange error from the correlation process. The group delay error is given by the root τ of the early/late gate error function [11]:

$$\begin{aligned} D(\tau) = &\left[R(\tau+\tau_d) - R(\tau-\tau_d)\right]\cos(\theta_c) \\ &+ \alpha\left[R(\tau+\tau_d-\delta) - R(\tau-\tau_d-\delta)\right]\cos(\theta_m - \theta_c) = 0 \end{aligned} \tag{A1}$$

where,

τ is the pseudorange multipath error (nsec)

τ_d is the early/late delay (1/2 C/A Code PRN chip = 489 nsec)

δ is the difference in path lengths, direct and reflected signals (nsec)

θ_c is the composite phase of the direct and reflected signal

θ_m is the multipath phase relative to the direct signal

α ratio of direct to reflected signal voltage $(0 \le \alpha \le 1)$

and,

$$R(\tau) = 1 - \frac{|\tau|}{T} \qquad |\tau| \le T$$

$$R(\tau) = 0 \qquad |\tau| > T$$

where,

T is the PRN C/A code bit period (978 nsec)

Depending on the level of the direct signal the amount of error introduced into the double difference computation can vary from 1 to 10 meters.

Table A1: Pseudorange Multipath Error

θ	δ (meters)	δ (nsec)	τ (meters) (-10 dB)	τ (meters) (-15 dB)
20	27	90	3	0.9
30	39	130	4	1.3
40	51	170	6	1.7
50	60	200	7	2
60	68	227	8	2.2

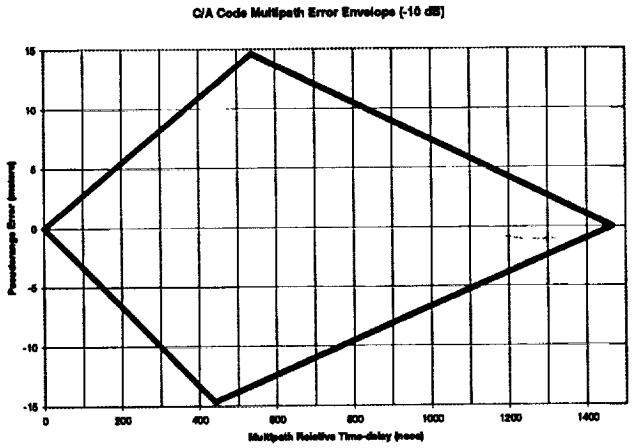

Figure A1: C/A Code Multipath Error Envelopes

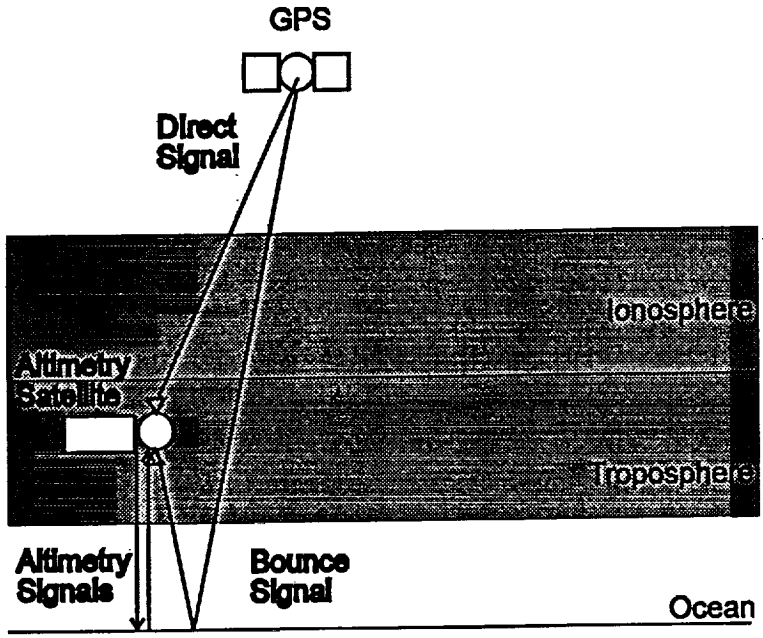

Figure 1A: Altimetry Satellite Signal Configuration

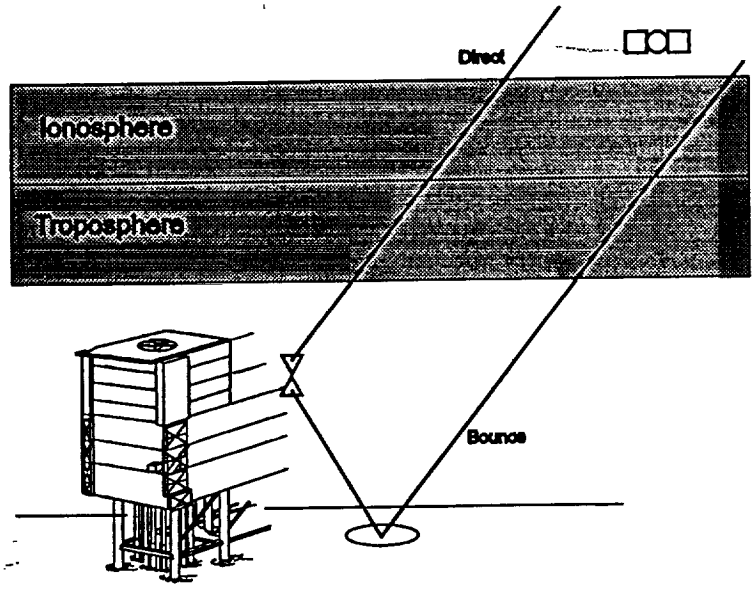

Figure 1B: Ground Experiment Signal Configuration

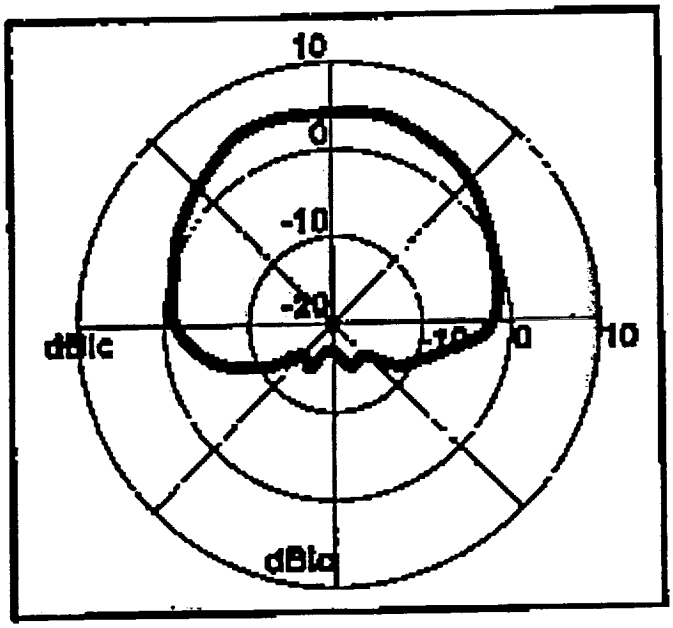

Figure 2A: RCP Antenna (Model 501) Gain Pattern With RCP Input

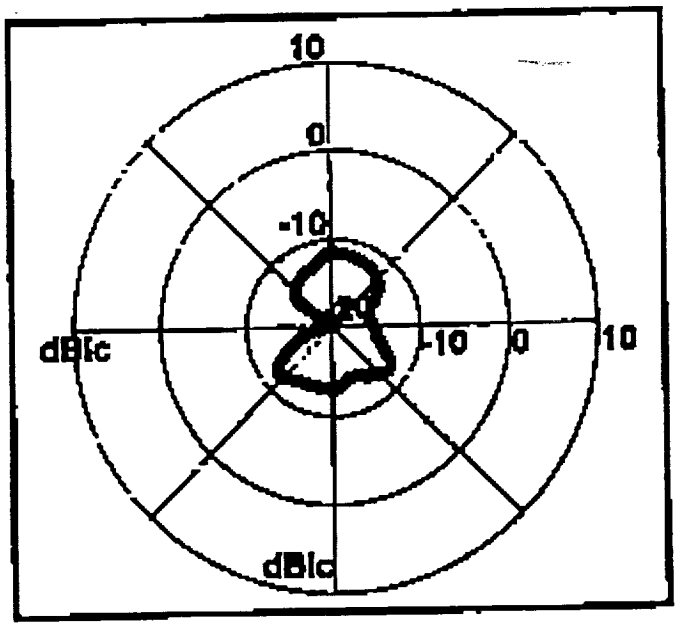

Figure 2B: RCP Antenna (Model 501) Gain Pattern With LCP Input
(Gain Patterns Provided By NovAtel Communications Ltd.)

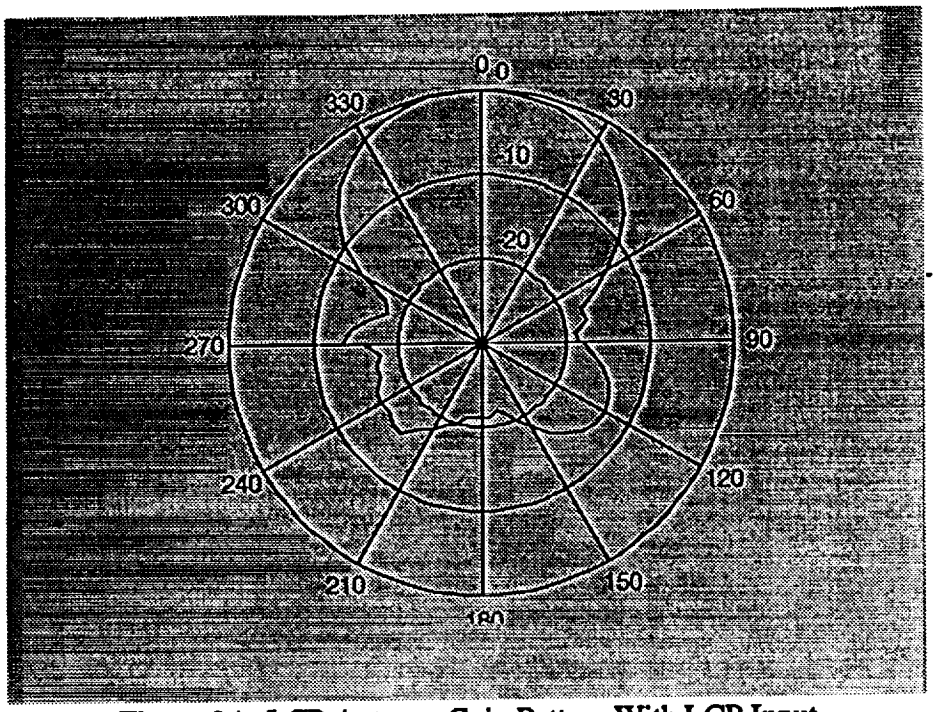

Figure 3A: LCP Antenna Gain Pattern With LCP Input

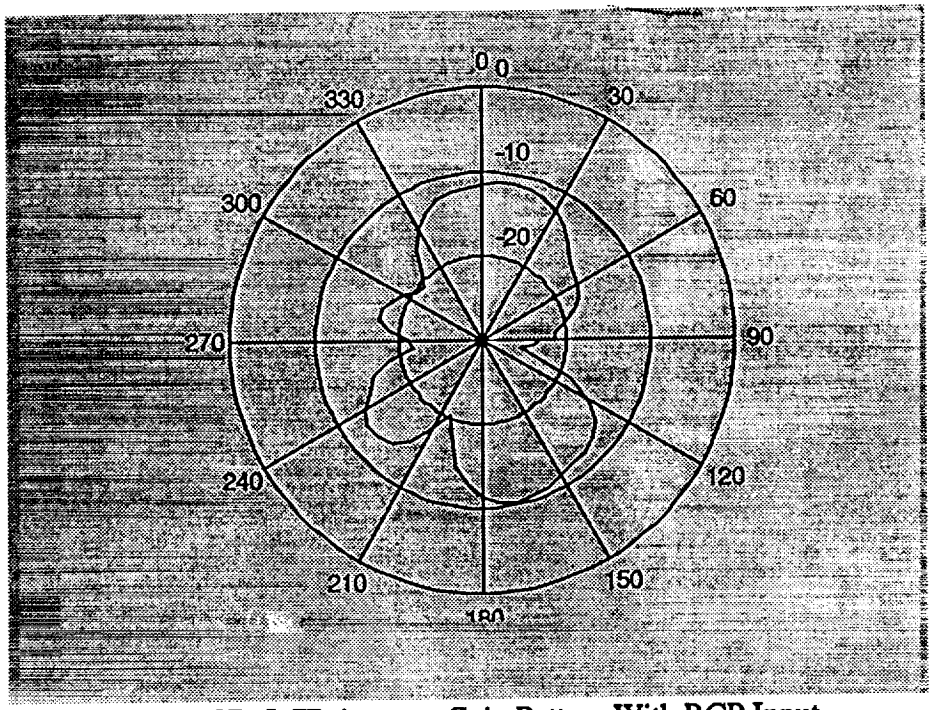

Figure 3B: LCP Antenna Gain Pattern With RCP Input

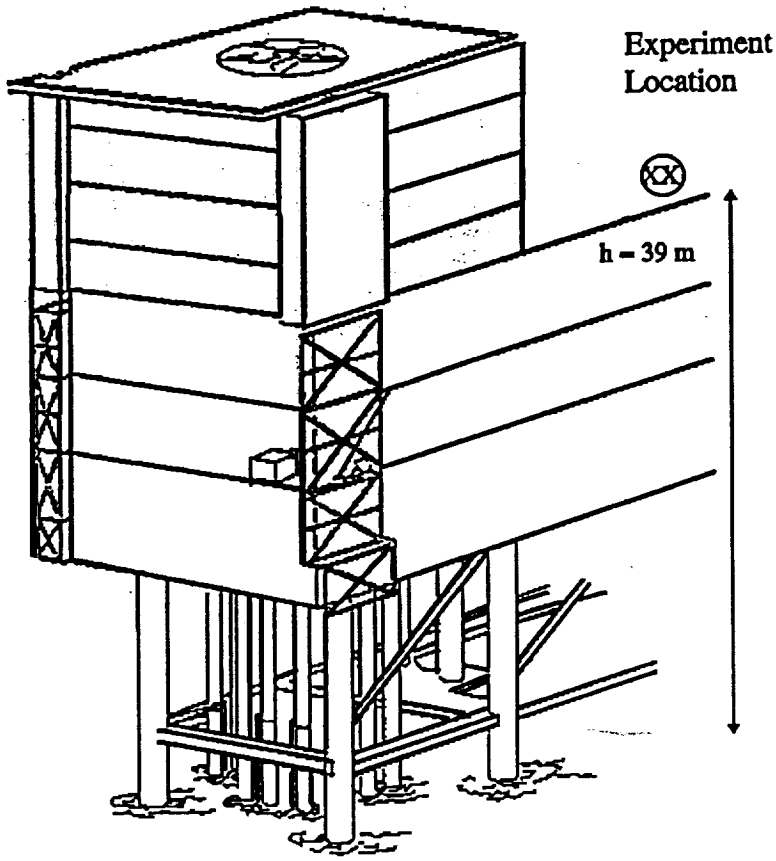

Figure 4: Harvest Platform

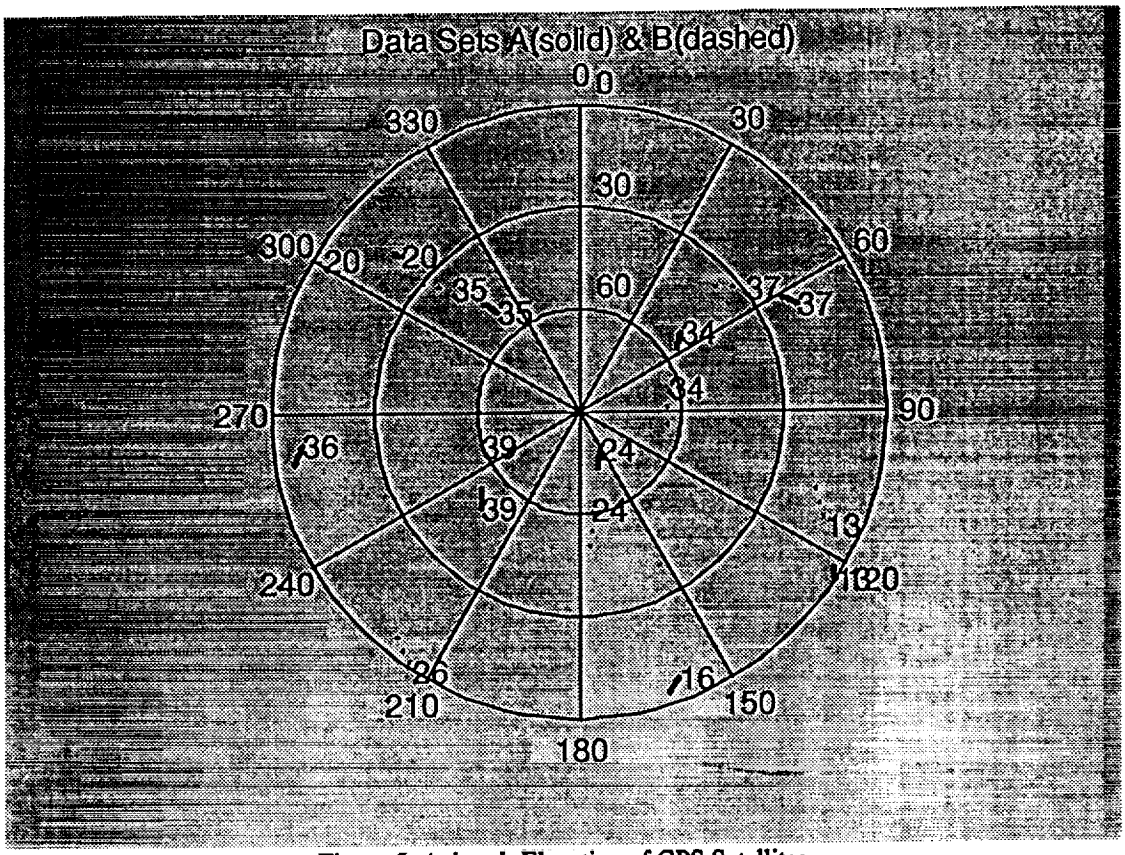

Figure 5: Azimuth-Elevation of GPS Satellites

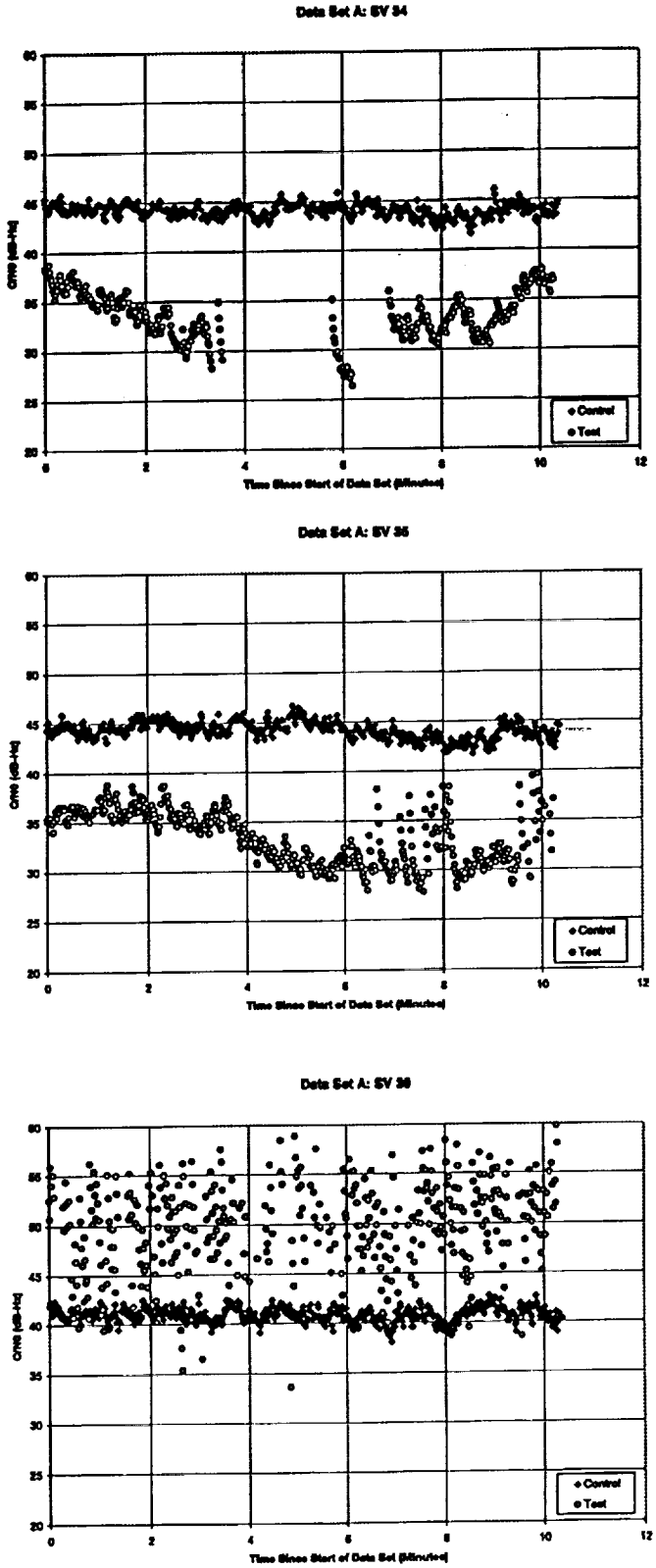

Figure 6: Carrier-to-Noise Ratios for Data Set A

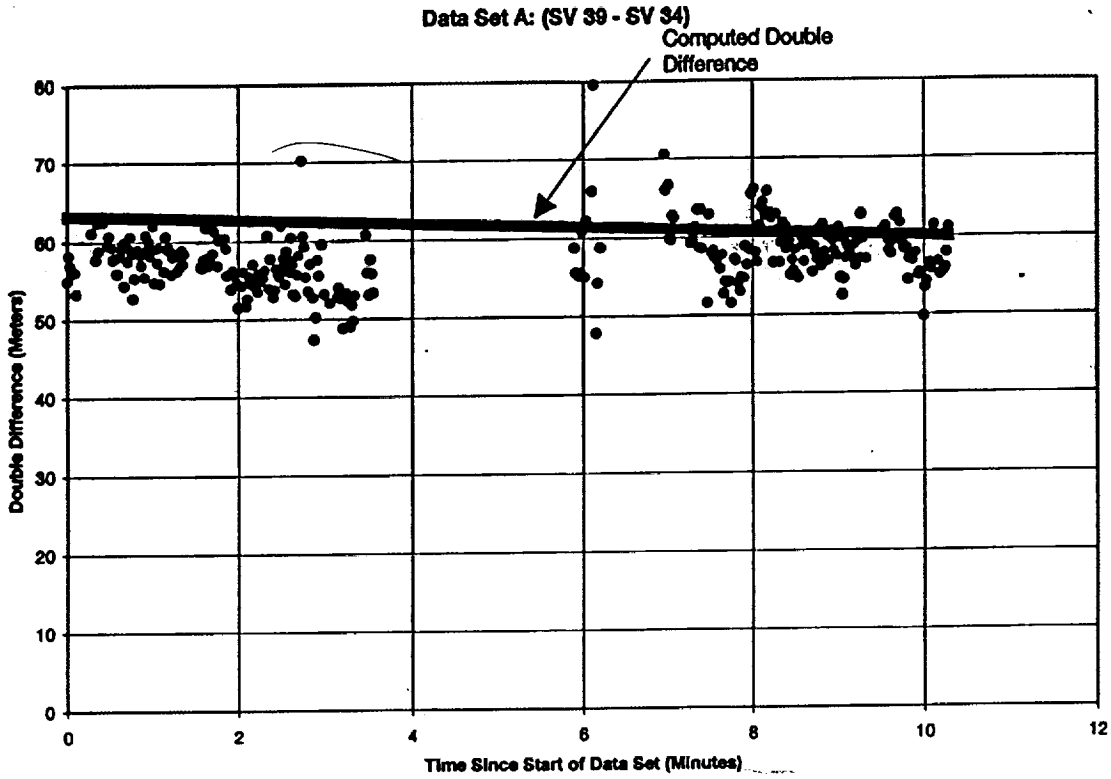

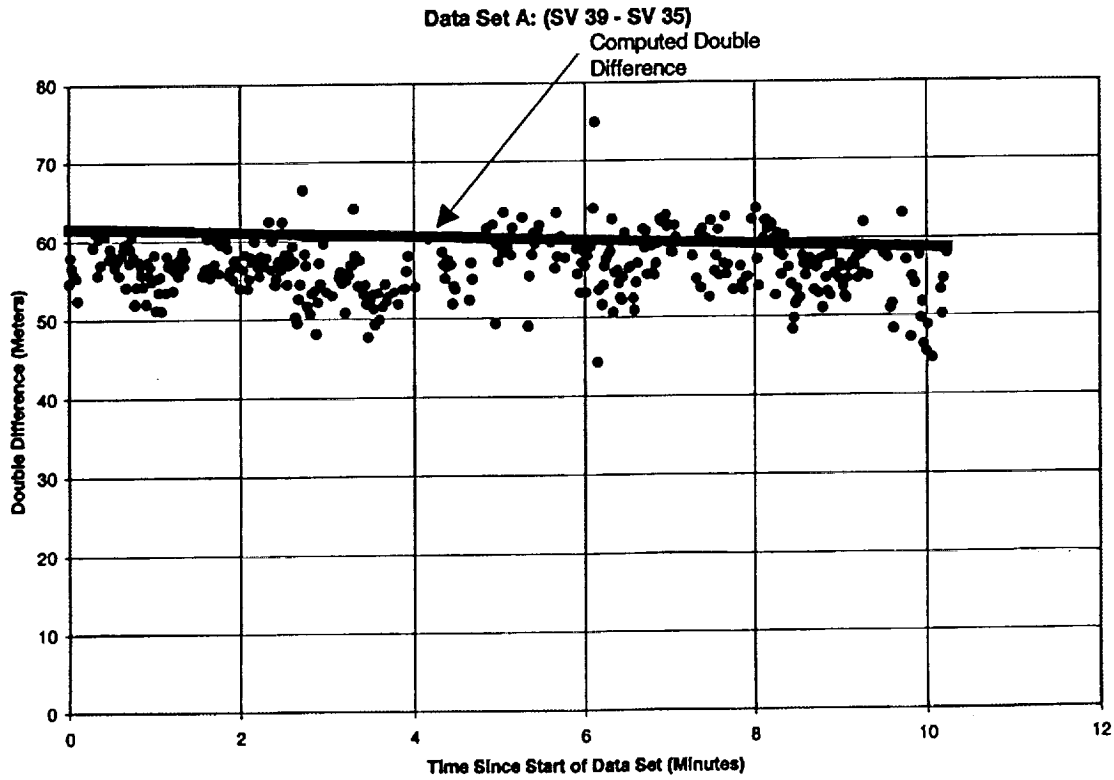

Figure 7: Double Differences for Data Set A

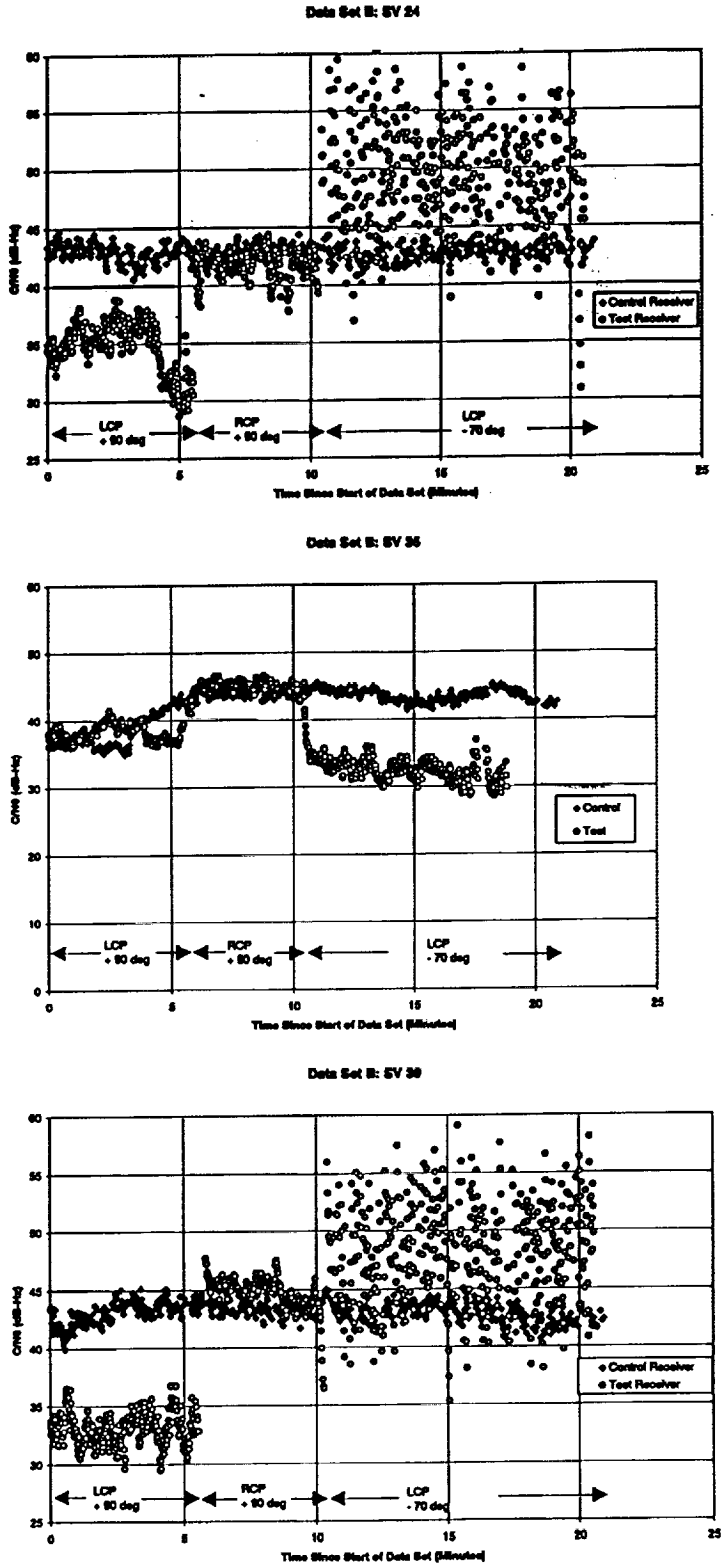

Figure 8: Carrier-to-Noise Ratios for Data Set B

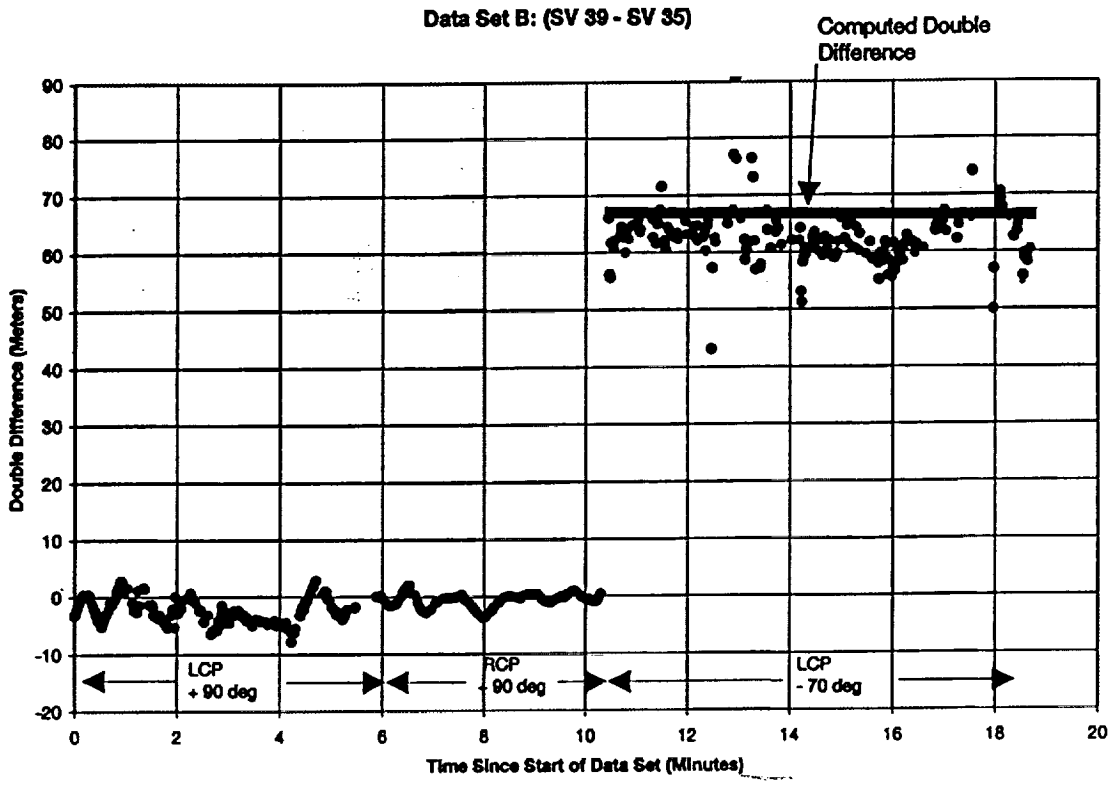

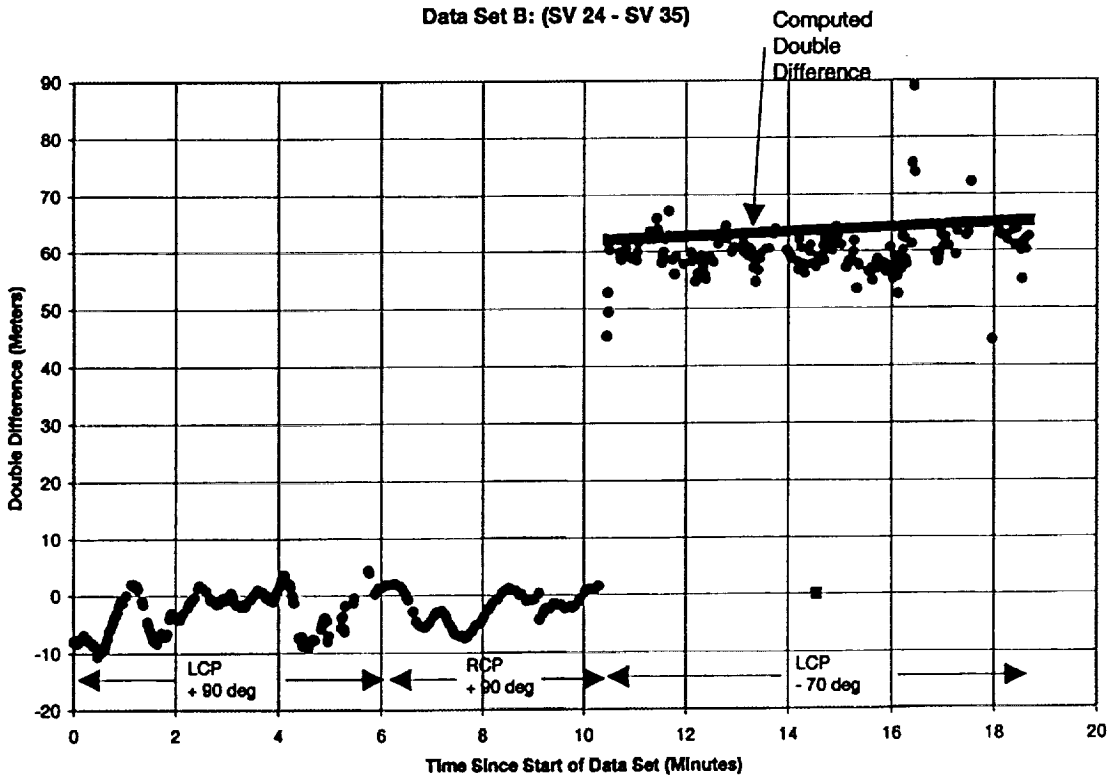

Figure 9: Double Differences for Data Set B